Effectiveness of Tuned Mass Dampers in Seismic Response Control of Isolated Bridges Including Soil-Structure Interaction

Abstract

The effect of soil-structure interaction (SSI) on the dynamic responses of seismically isolated three-span continuous reinforced concrete (RC) bridge is investigated. Also, tuned mass damper(s) (TMD/s) is/are installed to control undesirable bearing displacement, even under the SSI effect. The TMDs are placed at the midspan of the bridge and each tuned with a modal frequency, while controlling up to first few modes as desirable. The soil surrounding the foundation of pier is modeled by frequency independent coefficients. Dynamic analysis is carried out in time domain using direct integration method. In order to specify the effects of the SSI, the responses of the non-isolated, isolated, and controlled isolated bridge are compared. It is observed that the soil surrounding the pier has significant effects on the bearing displacement of the isolated RC bridges. In addition, it is observed that the seismic responses of isolated RC bridge reduced significantly with installation of the TMDs.

Keywords

Earthquake; isolated bridge; reinforced concrete (RC); SSI; tuned mass damper; TMD.

Said Elias [a, *]
Vasant Matsagar [b]

[a] Research Scholar, Indian Institute of Technology (IIT) Delhi, India, said.elias@civil.iitd.ac.in
[b] Associate Professor, Indian Institute of Technology (IIT) Delhi, India, matsagar@civil.iitd.ac.in

* Corresponding author

1 INTRODUCTION

Reinforced concrete (RC) bridges are the most important lifeline structures and their failure as a result of seismic incident seriously obstructs relief and rehabilitation work. There are number of bridges which have collapsed due to the past earthquakes, all over the world. Bridges are especially vulnerable to damage and can easily collapse as a result of earthquake ground motions; this is attributed to their structural simplicity (lesser redundancy) and the fundamental time period. The fundamental time period of vibration of most of the bridges is found to be in the range of 0.2 to 1 sec. From the past earthquakes, it is noted that the predominant time periods had been in this range, thereby it has caused the seismic response of bridges to amplify. The seismic response control achieved in the base-isolated bridge was studied by several researchers such as Jangid (2004),

Matsagar and Jangid (2006), Dicleli (2007), and Dicleli and Buddaram (2007). It was commonly found that the base isolation technique has been quite effective in seismic response mitigation of the bridges in reducing the pier base shear.

Earlier, the effectiveness of tuned mass dampers (TMDs) for vibration control of long-span bridges and tall buildings due to wind and earthquake excitations were extensively studied. Optimal linear vibration absorber for linear damped primary system was determined by Randall et al. (1981) using graphical solution. They reported that small offset in tuning of the frequency could result in decreased efficiency of a single TMD. The use of multiple tuned mass dampers (MTMDs) was also studied earlier amply, showing that the MTMDs are more effective than the single TMD (STMD). Daniel et al. (2012) studied the performance of the MTMDs in multi-mode response control of pedestrian bridges. They reported that the MTMDs improved the performance of the pedestrian bridges. Luu et al. (2012) have shown the effectiveness of the MTMDs to control the vibration of bridges caused due to trains moving at high speed. Matin et al. (2014 and 2017) reported that the TMDs are the best solution to control the bi-directional response of the concrete bridges subjected to earthquake ground excitations. Debnath et al. (2015) showed that the responses of the truss bridge were significantly reduced by adopting the multi-mode control approach. Later, Miguel et al. (2016) showed the improved performance of robust TMDs in response of bridges. Recently, Pisal and Jangid (2016) reported that placing all the multiple tuned mass friction dampers (MTMFDs) at the mid-span showed better performance as compared to the case wherein the devices are randomly placed along the span of the bridge.

The above mentioned studies, however, ignored the effect of soil-structure interaction (SSI), which is invariably present almost in all situations. Tongaonkar and Jangid (2003) reported that the soil surrounding the pier has significant effects on the response of the base-isolated bridges and under certain circumstances the bearing displacements at abutment locations may be underestimated if the SSI effects are not considered in the response analysis of the bridge system. Their investigation showed that consideration of the SSI in the analysis results in enhancement of safety and reduction in design costs. However, no study is seen yet by the authors wherein the TMDs have been installed in the isolated bridges with due consideration of the SSI effect. Hence, objectives of this study include studying: (i) the placement of the TMDs at mid-span of the RC bridge, and (ii) tuning of the TMDs to higher modal frequencies for seismic response mitigation of the base-isolated concrete bridge (IB) with considering of the SSI. The schemes compared in this study are: (i) installing a single TMD (STMD) on the IB (IB+STMD), (ii) installing two TMDs on the IB (IB+2TMDs), and (iii) installing three TMDs on the IB (IB+3TMDs).

2 MATHEMATICAL MODELING

In this study, three-span reinforced concrete (RC) bridge is considered as shown in Fig. 1. The assumptions made in developing the mathematical model are as follows:

1. The isolated bridge controlled with/ without TMDs systems are assumed to remain in elastic range.
2. The isolated bridges with/without TMDs are modeled as a finite element (FE) model divided into a number of small discrete segments (finite elements) and a node connects two adjacent segments together. Degrees of freedom (DoF) at each node are considered to be two and

masses of each segment are assumed to be distributed between the two adjacent nodes in the form of point masses.

(a)

(b)

(c)

Figure 1: (a) General elevation of three-span continuous concrete bridge, (b) Schematics of the TMD, (c) Finite element model of three-span continuous bridge with the SSI.

3. Mass contribution of the non-structural elements such as parapet walls, kerbs, and wearing coat is considered because they produce considerable inertial forces, however their stiffness is neglected.

4. The base-isolated bridge with/without TMDs is subjected to two horizontal (bi-directional) components of the ground motion and the effect of vertical component is not considered because the horizontal and vertical components of an earthquake are generally uncorrelated with it.

5. The soil supporting the pier foundation is modeled as spring and damper acting in the horizontal and rotational directions. Viscous damping is used to simulate the radiation damping

in the soil, which is developed through the loss of energy emanating from the foundation in the semi-infinite soil medium as per Tongaonkar and Jangid (2003).

6. The foundation is represented for all motions using a spring-dashpot-mass model with frequency-independent coefficients. The modeling of the foundation on deformable soil is performed in the same way as that of the structure and is coupled to perform a dynamic SSI analysis as per Tongaonkar and Jangid (2003).

7. Few selected modal responses are modified in the multi-mode control using the hybrid systems.

Fig. 1(a) shows the general elevation of a three-span continuous reinforced concrete (RC) bridge. The stiffness, $k_{i\text{-}x}$ and $k_{i\text{-}y}$; damping $c_{i\text{-}x}$ and $c_{i\text{-}y}$ of a TMD respectively in the longitudinal (N-S) and transverse (E-W) directions are shown in Fig. 1(b). Fig. 1(c) shows a finite element (FE) model of the base-isolated RC bridge installed with the TMDs, duly considering the flexibilities of both, the bridge deck and piers. The bridge bearings are supported on reinforced concrete piers and rigid abutments. The relative bearing displacement refers to the difference in displacement between the top and bottom cover plates of an isolator. The masses of the TMD are denoted by m_i ($i = 1$ to n) which are all installed at mid-span of the RC bridge. The bridge system has additional degrees-of-freedom at the base of the pier due to flexibility of foundation on which the bridge rests, i.e. SSI effects - refer degrees-of-freedom x_n and y_n in Fig. 1(c). The above assumptions facilitated the mathematical model of the bridge as shown in Fig. 1(c). A sufficiently accurate consideration of the soil behavior can be obtained if the soil stiffness and damping coefficients of a circular mass-less foundation on the soil strata are evaluated by the frequency independent expressions (Spyrakos, 1990). The stiffness and damping coefficients of the soil medium are expressed as follows.

$$K_s = \frac{8Ga}{2 - \upsilon}\left(1 + \frac{1}{2\overline{H}}\right) \text{ for } \overline{H} > 1 \tag{1}$$

$$K_r = \frac{8Ga^3}{3(2 - \upsilon)}\left(1 + \frac{1}{6\overline{H}}\right) \text{ for } 1 < \overline{H} \leq 4 \tag{2}$$

$$C_s = \frac{4.6Ga^2}{(2 - \upsilon)V_s} \tag{3}$$

$$C_r = \frac{0.4Ga^4}{(1 - \upsilon)V_s} \tag{4}$$

where stiffness of the swaying and rocking springs are represented respectively as K_s and K_r and the damping corresponding dashpots are indicated as C_s and C_r, respectively. G is the soil shear modulus; V_s is the shear wave velocity for soil; a is the radius of circular footing; υ is Poisson's ratio for the soil; H is the depth of the soil stratum overlying a rigid bedrock; and $\overline{H} = H/a$. The above expressions are also valid for the limiting case of a large soil stratum, in which the term $\overline{H}$ diminishes (Tongaonkar and Jangid, 2003). The equations of motion of the isolated bridge installed with the TMDs, under the two horizontal components of an earthquake ground motion expressed in matrix are,

$$[M_{\text{s}}]\{\ddot{Q}\} + [C_{\text{s}}]\{\dot{Q}\} + [K_{\text{s}}]\{Q\} = -[M_{\text{s}}]\{r\}\{\ddot{Q}_{\text{g}}\} \tag{5}$$

where $[M_{\text{s}}]$, $[C_{\text{s}}]$, and $[K_{\text{s}}]$ are the mass, damping, and stiffness matrices of the bridge, respectively of order $(2N + 2n + 2n_{\text{b}} + n_{\text{s}}) \times (2N + 2n + 2n_{\text{b}} + n_{\text{s}})$; N, n, n_{b}, and n_{s} indicate the degrees of freedom of the bridge, the TMDs, isolators, and soil, respectively; $\{Q\} = \{X_1, X_2, \ldots X_N, x_{1\text{b}} \ldots x_{n\text{b}}, x_1 \ldots x_n, x_{\text{s}}, x_\theta, Y_1, Y_2, \ldots Y_N, y_{1\text{b}} \ldots y_{n\text{b}}, y_1 \ldots y_n, y_{\text{s}}, y_\theta\}^{\text{T}}$, $\{\dot{Q}\}$, and $\{\ddot{Q}\}$ are the displacement, velocity, and acceleration vectors, respectively; $\{\ddot{Q}_{\text{g}}\}$ is the earthquake ground acceleration vector, including $\ddot{x}_{\text{g}}$ and $\ddot{y}_{\text{g}}$ as the earthquake ground acceleration in the longitudinal: N-S and transverse: E-W directions, respectively; and $\{r\}$ is the vector of influence coefficients. Further, $\{X_i\}$ and $\{Y_i\}$ are the displacements of the ith node of the bridge in the N-S and E-W directions, respectively. The isolation system is considered by the parameters namely: the lateral stiffness (k_{b}) and the damping constant (c_{b}) as shown in Fig. 1(c). The elastomeric bearings for the above bridges are designed to provide the specified values of two parameters namely, the time period of isolation of the bearings, T_{b} and the viscous damping ratio, ζ_{b} expressed as,

$$\sum k_{\text{b}} T_{\text{b}}^2 = 4 M_{\text{d}} \pi^2 \tag{6}$$

$$\sum c_{\text{b}} = 2\zeta_{\text{b}} M_{\text{d}} \omega_{\text{b}} \tag{7}$$

where M_{d} is the mass of the bridge deck; $\sum k_{\text{b}}$ is the total stiffness of the bearings; $\sum c_{\text{b}}$ is the total viscous damping of the bearings; and $\omega_{\text{b}} = 2\pi / T_{\text{b}}$ is the isolation frequency.

Earthquake ground motion often excites several vibration modes of the bridges, which may especially lead to increased displacement. Due to this effect, the bridge can be damaged, unseating of deck may occur and it may deem unsafe for riding, which is abruption of the vital lifeline. Therefore, the dynamic response in the first few modes of the isolated bridge can be controlled in both, longitudinal and transverse directions simultaneously, for which the frequency of each TMD can be calculated as,

$$f_{\text{i-x}} = \frac{\omega_{\text{i-x}}}{\Omega_{\text{i-x}}}; \quad i = 1 \text{ to } n \tag{8-a}$$

$$f_{\text{i-y}} = \frac{\omega_{\text{i-y}}}{\Omega_{\text{i-y}}}; \quad i = 1 \text{ to } n \tag{8-b}$$

where the tuning frequency ratios are: $f_{\text{i-x}} = 1$ and $f_{\text{i-y}} = 1$, respectively in the N-S and E-W directions. Here, $\omega_{\text{i-x}}$ and $\Omega_{\text{i-x}}$ respectively are the frequencies of the TMDs and first few natural frequencies of the isolated bridge in the longitudinal (N-S) direction. The frequencies of the TMDs and first few natural frequencies of the isolated bridge in the transverse (E-W) direction respectively are $\omega_{\text{i-y}}$ and $\Omega_{\text{i-y}}$. The effectiveness of the TMDs can be improved by suitably designing parameters of the TMDs as,

$$k_{i\text{-}x} = \frac{m_t}{\left(\dfrac{1}{\omega_{1\text{-}x}^2} + \dfrac{1}{\omega_{2\text{-}x}^2} + \cdots + \dfrac{1}{\omega_{n\text{-}x}^2}\right)} \qquad i = 1 \text{ to } n \tag{9-a}$$

$$k_{i\text{-}y} = \frac{m_t}{\left(\dfrac{1}{\omega_{1\text{-}y}^2} + \dfrac{1}{\omega_{2\text{-}y}^2} + \cdots + \dfrac{1}{\omega_{n\text{-}y}^2}\right)} \qquad i = 1 \text{ to } n \tag{9-b}$$

Then total mass of all the TMDs (m_t) is calculated from the known total mass of the bridge deck (M_t) and an assumed total mass ratio μ. The mass ratio defines relative weights of the TMDs as compared to the bridge deck, which can be determined for maximizing the dynamic response reduction achieved. Subsequently, the masses of each TMD unit are calculated as,

$$m_{i\text{-}x} = \frac{k_{i\text{-}x}}{\omega_{i\text{-}x}^2} \qquad i = 1 \text{ to } n \tag{10-a}$$

$$m_{i\text{-}y} = \frac{k_{i\text{-}y}}{\omega_{i\text{-}y}^2} \qquad i = 1 \text{ to } n \tag{10-b}$$

The damping ratios ($\zeta_d = \zeta_1 = \zeta_2 = \cdots = \zeta_n$) of the TMDs are kept the same and the damping ($c_{n,i}$) of the TMDs are calculated as,

$$c_{i\text{-}x} = 2\zeta_d m_i \omega_{i\text{-}x} \quad i = 1 \text{ to } n \tag{11-a}$$

$$c_{i\text{-}y} = 2\zeta_d m_i \omega_{i\text{-}y} \quad i = 1 \text{ to } n \tag{11-b}$$

The dynamic properties of the TMDs can be suitably optimized to achieve highest seismic response reduction. Newmark's- β step-by-step method of time integration is used to solve the governing equations of motion (Equation 5) for all the cases considered in this study. Combined MATLAB and SAP2000 simulations are used for modeling, verification, and validation of numerical results obtained for the different bridge models used in this study along with the seismic response controllers.

3 NUMERICAL STUDY

The seismic response control of an isolated three-span continuous reinforced concrete (RC) bridge with piers and a box girder is investigated under bi-directional components of three different real earthquake ground motions. Ribes-Llario et al. (2016) reported that for higher excitation frequency, increased accelerations are induced, which consequently increases pier base shear. Therefore, in this study three earthquakes namely, Imperial Valley, 1940; Northridge, 1994; and Kobe, 1995 are considered with relatively high excitation frequency contents. Imperial Valley, 1940 earthquake was recorded at El Centro station in the USA; Northridge, 1994 earthquake was recorded at Channel station in the USA; and Kobe, 1995 earthquake was recorded at the Japan Meteorological Agency - JMA station in Japan. They respectively have peak ground acceleration (PGA) of 0.21g, 0.58g, and

0.86g in the longitudinal direction; and 0.34g, 0.55g, and 0.82g in the transverse direction, where g denotes the gravitational acceleration. The fast Fourier transform (FFT) of the earthquake ground motions are shown in Fig. 2. These earthquake ground motions are mostly recoded at the near-fault locations with rocky terrain. Furthermore, they have notably high frequency content as seen in Fig. 2. The FFT amplitudes corresponding to the higher frequencies may be detrimental to the bridge causing more seismic damage.

The properties of this bridge system are taken from the bridge studied by Tongaonkar and Jangid (2003). The geometric and material properties of this bridge are given in Table 1. The structure is assumed to consist of a series of beam elements used to model the bridge deck and bridge piers. The bridge piers are divided in to five nodes which contains ten degrees of freedom in each horizontal direction. In addition, the deck of each span is divided into five nodes. Thus, flexibility of both, the piers and deck has been duly modeled. The total degrees of freedom in each direction are 20. The fundamental periods of the fixed-base RC bridge in both directions are 0.53 sec with damping ratio of 5%. The other subsequent lower modal time periods of the structure in both, longitudinal and transverse directions respectively are: 0.49, 0.25, and 0.15 sec; and 0.47, 0.24, and 0.16 sec.
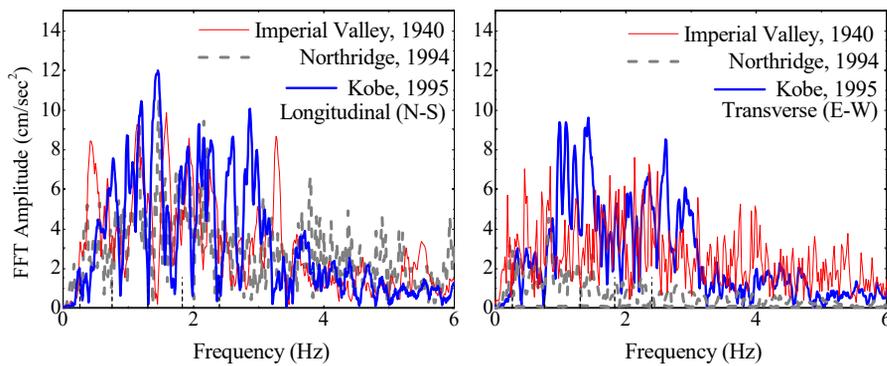
Figure 2: The fast Fourier transforms (FFTs) of the bi-directional earthquake ground motions.

Member Properties of the RC Bridge	Deck	Piers
Cross-sectional area (m^2)	3.57	1.767
Moment of inertia in N-S direction (m^4)	2.08	0.902
Moment of inertia in E-W direction (m^4)	2.08	0.902
Young's modulus of elasticity (kN/m^2)	3.6×10^7	3.6×10^7
Mass per unit volume (kN/m^3)	23.536	23.536
Length or height (m)	3@30 = 90	10
Shape	Square	Circular

Table 1: Geometric and material properties of the reinforced concrete (RC) bridge.

Here, base isolation and tuned mass dampers (TMDs) are used together in the bridges with an objective of reducing their seismic response through the hybrid control. The TMDs designed to control the modal responses of the RC bridge in both the horizontal (longitudinal and transverse)

directions. In this work, the single mass of the TMD is considered to be connected to the bridge deck by using two separate springs and dashpots in the two horizontal directions, thereby providing independent design frequencies in each direction. In all cases of the IB, IB+STMD, IB+2TMDs, and IB+3TMDs, the parameters for the isolators are designed by using Equations 6 and 7, where isolation time period is taken as $T_b = 2$ sec; and damping ratio of $\zeta_b = 0.125$.

The SSI effect is included to assess the performance of the TMDs. Three types of the soil properties are considered, which are hard soil, medium soil, and soft soil. The shear wave velocity (V_s), shear modulus (G), and other dynamic properties of different types of soil are given in Table 2, which are taken from the study reported by Tongaonkar and Jangid (2003). Also, Poisson's ratio (υ) is taken 0.4. The TMDs are designed for the RC bridge with rigid foundation as per their design parameters given in Table 3. The TMDs are designed with same damping ratio of 5% as of the bridge. The mass ratios (1%) for the different TMD schemes are kept the same for comparisons purpose. The response quantities of the bridge in the longitudinal as well as transverse direction are plotted for the base-isolated RC bridge, controlled with the STMD, 2TMDs placed at the mid-spans, and 3TMDs placed at the mid-spans. It is to be noted that the STMD, 2TMDs, and 3TMDs are installed in each span of the RC bridge. The modal time periods of the base-isolated bridge while considering the SSI in the longitudinal (N-S) and transverse (E-W) directions for the rigid, hard, medium, and soft soils in the cases studied here are presented in Table 4.

It is to be noted that the TMDs in IB+2TMDs and IB+3TMDs cases are designed such that the shift in the frequencies in all the three schemes remain insignificant. This criterion is mainly considered for the comparison of the performance of the TMD schemes.

Properties of Soil	Hard Soil	Medium Soil	Soft Soil
Shear modulus, G (MPa)	3.57	0.357	0.179
Shear wave velocity, V_s (m/s)	394	134	99.6
Translational stiffness of soil medium, K_s (10^8 N/m)	4.29	0.429	0.214
Rocking stiffness of soil medium, K_r (10^8 Nm)	1.8	0.18	0.09
Translational damping coefficient, C_s (10^7 N-s/m)	1.04	0.307	0.206
Rocking damping coefficient, C_r (10^7 Nm-s)	0.967	0.285	0.191

Table 2: Dynamic properties of different types of soil.

Schemes	TMDs	Frequency, ω_i (rad/sec)		Mass, m_i (ton)		Stiffness, k_i (kN/m)		Damping, c_i ($kN\ sec/m$)	
		N-S	E-W	N-S	E-W	N-S	E-W	N-S	E-W
STMD	TMD-1	3.00	3.00	92.79 (1% of M_t)		840.50	8405.00	28.00	28.00
2TMDs	TMD-1	3.00	3.00	92.30	73.34	836.00	665.00	27.69	22.00
	TMD-2	42.00	5.84	0.50	19.46	836.00	665.00	2.10	11.36
3TMDs	TMD-1	3.00	3.00	91.90	68.30	833.00	618.00	27.57	20.49
	TMD-2	42.00	5.84	0.47	18.20	833.00	618.00	1.97	10.63
	TMD-3	45.00	9.86	0.40	6.50	833.00	618.00	1.80	6.41

Table 3: Design parameters for the STMD and TMDs in the base-isolated RC bridge.

Base Condition	Time Periods of the Isolated Bridge in Different Modes							
	IB		IB+STMD		IB+2TMDs		IB+3TMDs	
Mode	N-S	E-W	N-S	E-W	N-S	E-W	N-S	E-W
Rigid foundation 1	2.0	2.0	2.3	2.3	2.3	2.278	2.3	2.25
2	0.149	1.074	2.09	2.1	2.092	2.1	2.092	2.089
3	0.13	0.639	2.087	2.093	2.09	2.092	2.088	2.088
4	0.077	0.465	1.9	1.896	1.91	1.92	1.89	1.88
Hard soil 1	2.1	2.1	2.35	2.31	2.353	2.29	2.355	2.28
2	0.261	1.075	2.094	2.1	2.092	2.1	2.099	2.095
3	0.26	0.639	2.09	2.097	2.09	2.092	2.091	2.089
4	0.149	0.465	1.94	1.91	1.94	1.93	1.9	1.88
Medium soil 1	2.88	2.3	3.0	2.447	2.98	2.43	3.0	2.425
2	0.583	1.094	2.092	2.11	2.092	2.1	2.092	2.091
3	0.57	0.679	2.092	2.097	2.092	2.092	2.088	2.089
4	0.149	0.67	2.025	1.965	2.026	1.985	2.01	1.94
Soft soil 1	3.55	3.46	3.62	3.58	3.62	3.569	3.64	3.55
2	0.68	1.119	2.092	2.11	2.092	2.1	2.091	2.092
3	0.656	0.816	2.092	2.098	2.092	2.092	2.091	2.09
4	0.149	0.815	2.042	1.99	2.043	2.01	2.048	1.89

Table 4: Effect of hybrid control systems and SSI on the modal time periods of the bridge structure.

3.1 Effectiveness of the TMDs

In this section, the performance of the TMD schemes in dynamic response control of the isolated RC bridge is investigated. The variation of normalized pier base shear, deck acceleration, and isolator displacement in longitudinal and as well transverse directions with varying the soil type under different real earthquake are plotted in Figs. 3 through 6.

In addition, the comparisons of the performance of hybrid controller schemes such as IB+STMD, IB+2TMDs, and IB+3TMDs in response control of isolated bridge (IB) are shown. It is observed that the SSI affects the displacements of the bearings. It is noticed from the trends in these figures that in the longitudinal direction (N-S), the peak bearing displacements at the abutment location reduced by 30%, when the effects of the SSI are considered for the isolated bridge (IB).

Also, bearing displacements at the pier location are found to decrease from 0.31 m to 0.22 m, i.e. when the effects of the SSI are considered in the IB case. On the other hand, in the transverse direction (E-W), the peak bearing displacement at the abutment location for the isolated bridge is found to be increased by 20%. In addition, the bearing displacements at the pier location are found to decrease from 0.18 m to 0.16 m, i.e. when the effects of the SSI are considered. Thus, the bearing displacement at the abutment increases, whereas at the pier location it decreases due to the SSI effects. This means that the design bearing displacements at the abutment may be underestimated if the effects of the SSI are ignored for the design of the base-isolated RC bridge. The bearing displacement at the pier location decreased mainly due to the soil flexibility. However, the bearing displacement increased at the abutment location as the relative and absolute displacements are almost the same there. It is therefore, proposed to install the TMDs to improve the performance of the base-isolated bridge duly accounting for the SSI effects. Generally, it is seen that installing the

STMD on the base-isolated bridge (IB+STMD) the undesirable bearing displacement tends to reduce both at the abutment and pier locations. However, it is seen that the STMD designed as per the frequency of the bridge with rigid foundation may not show significantly improved seismic performance for the bridge considering the SSI effect. Further, it is noticed that the nTMDs have showed more effectiveness in the response control of the base-isolated bridge. Generally, the responses are considerably reduced as compared to those of the bridge without the TMD, IB, and IB+STMD. It implies that all the TMD schemes are effective in response reduction of the base-isolated RC bridges under the earthquake-induced forces.
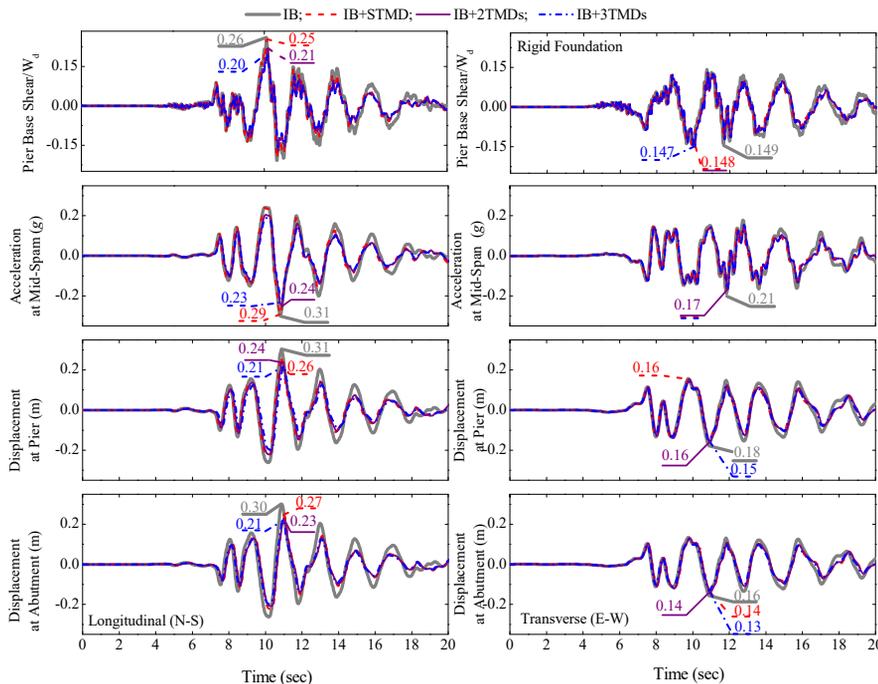
Figure 3: Time variation of pier base shear, deck acceleration, and isolator displacements for bridge with rigid foundation under Kobe ground motion in longitudinal and transverse directions ($T_b = 2$ sec; $\zeta_b = 0.125$).

It is noticed that with increasing flexibility of the foundation, the normalized peak pier base shear and deck acceleration are reduced significantly. Also, the performance of the STMD is observed to be insignificant due to off-tuning (mismatch of frequencies) that occurs due to the SSI effect. It is concluded that the isolator displacement at the abutment location increased significantly in the base-isolated RC bridge by considering the SSI. In addition, significant reduction in the isolator displacement is achieved by installing the TMDs. Further, base shear and deck acceleration reduced significantly in both the directions after installation of the STMD and TMDs. Moreover, the soil type greatly affects the performance of the bridge with the STMD and nTMDs schemes and seismic responses of the bridge with flexible foundation. Hence, the effects of the SSI are important to be considered especially in the bridge structure where TMD(s) is/are intended to be installed for seismic response reduction purpose. It is seen that the post-peak response reduces substantially when the TMDs are installed as compared to the uncontrolled fixed-base bridge or the isolated bridge controlled STMD cases.
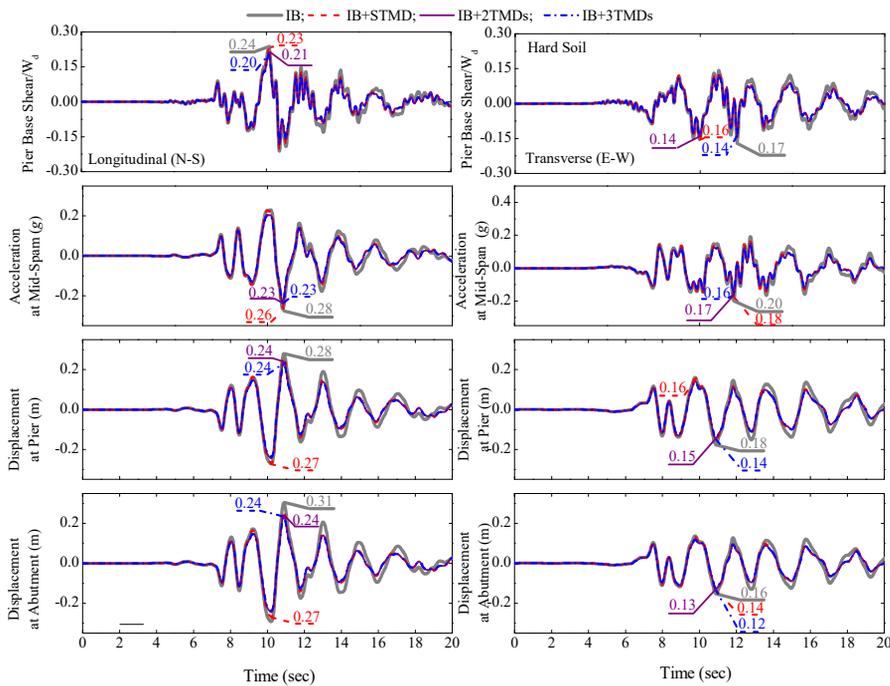
Figure 4: Time variation of pier base shear, deck acceleration, and isolator displacements for bridge with hard soil foundation under Kobe ground motion in longitudinal and transverse directions ($T_b = 2$ sec; $\zeta_b = 0.125$).
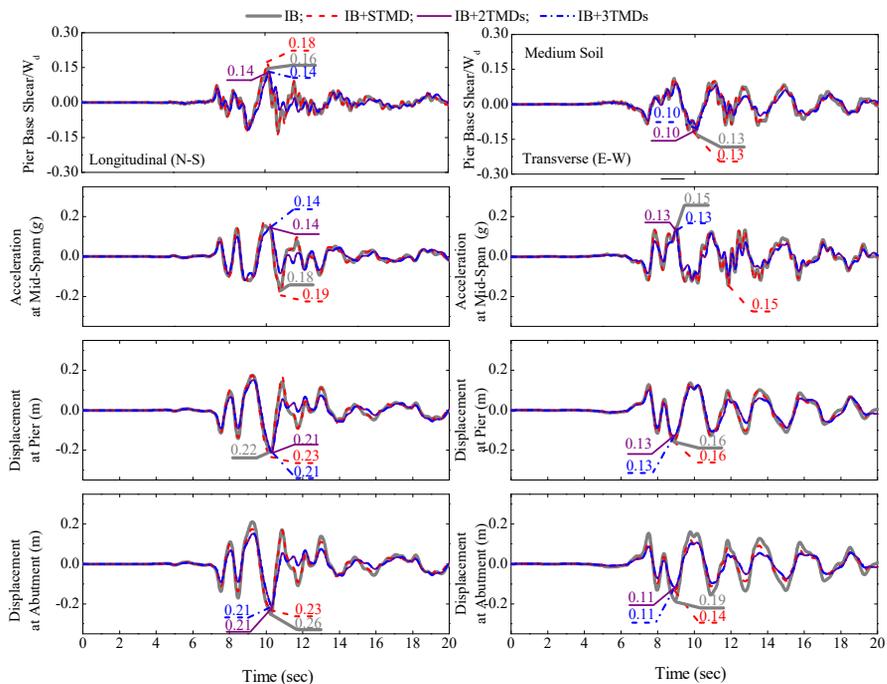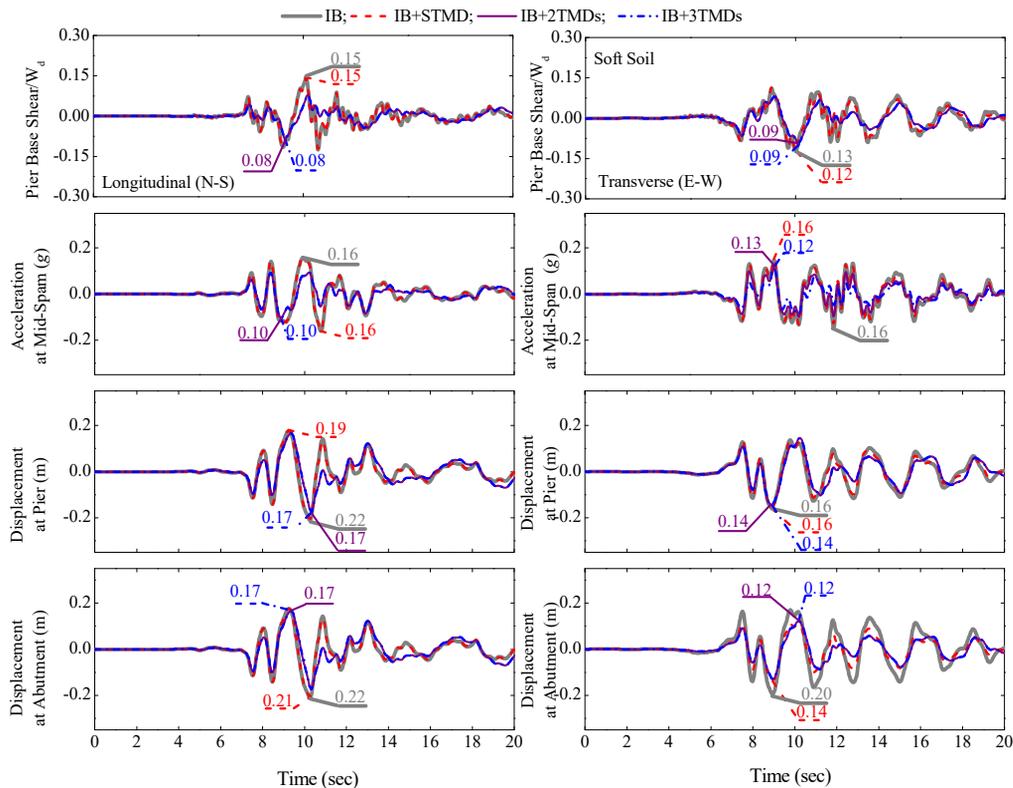

Figure 5: Time variation of pier base shear, deck acceleration, and isolator displacements for bridge with medium soil under Kobe ground motion in longitudinal and transverse directions ($T_b = 2$ sec; $\zeta_b = 0.125$).

Figure 6: Time variation of pier base shear, deck acceleration, and isolator displacements for bridge with soft soil under Kobe ground motion in longitudinal and transverse directions (T_b = 2 sec; ζ_b = 0.125).

3.2 Parameters Affecting the Design of the TMDs

In this section, the detailed parametric studies are conducted to evaluate and compare the seismic performance of different controller schemes explained in the aforementioned sections. The pier base shear normalized by the deck weight, $W_d = M_d \times g$, where M_d is the mass of the deck and g is the gravitational acceleration, acceleration at mid-span, displacement at pier and abutment are tabulated in Tables 5 through 8.

The comparison of the seismic performance of the different controller schemes for the bridge with rigid foundation under the Imperial Valley, 1940; Northridge, 1994; and Kobe, 1995 earthquakes are presented in Table 5. In addition, the isolator flexibility is increased to verify the effect of variation in the isolator flexibility on the performance of the TMD schemes. It is generally noticed that the TMD schemes are able to control the seismic responses of the isolated bridge. In addition, it is observed that TMDs are more effective in the cases where the isolator flexibility (T_b) is increased. The reduction in the displacement could be enhanced by applying some optimization technique to obtain optimum parameters of the TMD schemes. The design parameters (Table 4) are chosen such that the displacement reduces and at the same time the other seismic responses must not be magnified.

Responses under Ground Motions		T_b	Base-Isolated Bridge with								Fixed-Base	
			IB		IB+STMD		IB+2TMDs		IB+3TMDs			
			N-S	E-W	N-S	E-W	N-S	E-W	N-S	E-W	N-S	E-W
Imperial Valley, 1940	Pier Base Shear/W_d	2	0.117	0.126	0.10	0.11	0.090	0.095	0.087	0.091		
		2.5	0.100	0.124	0.08	0.10	0.075	0.079	0.071	0.066	0.705	0.996
		3	0.111	0.100	0.09	0.08	0.080	0.065	0.067	0.056		
	Acceleration at Mid-Span (g)	2	0.118	0.169	0.10	0.145	0.085	0.131	0.082	0.128		
		2.5	0.116	0.160	0.10	0.138	0.088	0.125	0.084	0.123	0.671	0.903
		3	0.117	0.145	0.10	0.125	0.089	0.118	0.085	0.117		
	Displacement at Pier (m)	2	0.084	0.100	0.08	0.09	0.07	0.075	0.068	0.071		
		2.5	0.125	0.160	0.11	0.12	0.11	0.115	0.105	0.098	0	0
		3	0.200	0.180	0.16	0.14	0.125	0.128	0.121	0.111		
	Displacement at Abutment (m)	2	0.085	0.106	0.08	0.100	0.07	0.085	0.063	0.078		
		2.5	0.130	0.150	0.12	0.140	0.105	0.128	0.095	0.118	0	0
		3	0.205	0.175	0.18	0.155	0.161	0.148	0.145	0.137		
Northridge, 1994	Pier Base Shear/W_d	2	0.21	0.093	0.18	0.085	0.168	0.078	0.162	0.075		
		2.5	0.17	0.085	0.16	0.079	0.145	0.069	0.141	0.065	1.439	0.824
		3	0.145	0.095	0.13	0.082	0.124	0.072	0.122	0.069		
	Acceleration at Mid-Span (g)	2	0.238	0.141	0.22	0.132	0.205	0.125	0.201	0.118		
		2.5	0.198	0.111	0.18	0.085	0.173	0.082	0.168	0.078	1.396	0.822
		3	0.166	0.091	0.16	0.082	0.155	0.077	0.145	0.069		
	Displacement at Pier (m)	2	0.17	0.051	0.12	0.045	0.115	0.042	0.111	0.041		
		2.5	0.205	0.055	0.18	0.048	0.173	0.044	0.168	0.042	0	0
		3	0.240	0.063	0.21	0.052	0.195	0.048	0.188	0.045		
	Displacement at Abutment (m)	2	0.172	0.046	0.16	0.041	0.148	0.038	0.141	0.035		
		2.5	0.188	0.053	0.18	0.049	0.169	0.043	0.159	0.041	0	0
		3	0.211	0.061	0.20	0.053	0.188	0.048	0.175	0.045		
Kobe, 1995	Pier Base Shear/W_d	2	0.26	0.149	0.25	0.148	0.21	0.148	0.20	0.147		
		2.5	0.125	0.122	0.12	0.115	0.11	0.11	0.10	0.10	3.034	1.833
		3	0.112	0.128	0.10	0.11	0.09	0.10	0.09	0.09		
	Acceleration at Mid-Span (g)	2	0.31	0.21	0.29	0.17	0.24	0.17	0.23	0.17		
		2.5	0.285	0.175	0.26	0.15	0.23	0.13	0.22	0.12	2.903	1.719
		3	0.236	0.138	0.21	0.12	0.19	0.11	0.18	0.10		
	Displacement at Pier (m)	2	0.31	0.18	0.26	0.16	0.24	0.16	0.21	0.15		
		2.5	0.38	0.237	0.29	0.18	0.26	0.17	0.24	0.16	0	0
		3	0.44	0.298	0.36	0.22	0.33	0.19	0.30	0.18		
	Displacement at Abutment (m)	2	0.30	0.16	0.27	0.14	0.23	0.14	0.21	0.13		
		2.5	0.369	0.221	0.33	0.19	0.27	0.17	0.26	0.16	0	0
		3	0.425	0.245	0.38	0.20	0.33	0.19	0.31	0.18		

Table 5: Peak response quantities for the RC bridge with different controller schemes for rigid foundation condition.

The selected design parameters facilitated the TMD schemes to reduce the base shear and deck acceleration. Additionally, it is seen that the performance of the multiple TMDs is better as compared to the case of the STMD.

Responses under Ground Motions		Base-Isolated Bridge with									Fixed-Base	
		IB		IB+STMD		IB+2TMDs		IB+3TMDs				
		T_b	N-S	E-W	N-S	E-W	N-S	E-W	N-S	E-W	N-S	E-W
Imperial Valley, 1940	Pier Base Shear/W_d	2	0.111	0.126	0.095	0.115	0.088	0.103	0.086	0.098		
		2.5	0.095	0.122	0.085	0.109	0.079	0.095	0.071	0.086	0.619	0.772
		3	0.100	0.095	0.088	0.088	0.082	0.081	0.077	0.075		
	Acceleration at Mid-Span (g)	2	0.119	0.160	0.105	0.145	0.095	0.138	0.089	0.133		
		2.5	0.117	0.140	0.101	0.125	0.087	0.122	0.081	0.119	0.669	0.836
		3	0.115	0.130	0.098	0.115	0.079	0.111	0.075	0.098		
	Displacement at Pier (m)	2	0.079	0.098	0.071	0.086	0.065	0.079	0.060	0.071		
		2.5	0.118	0.111	0.106	0.100	0.100	0.088	0.097	0.082	0	0
		3	0.173	0.165	0.165	0.148	0.148	0.139	0.141	0.133		
	Displacement at Abutment (m)	2	0.094	0.108	0.085	0.089	0.078	0.075	0.075	0.071		
		2.5	0.140	0.158	0.129	0.142	0.119	0.136	0.105	0.128	0	0
		3	0.215	0.185	0.188	0.169	0.169	0.158	0.159	0.138		
Northridge, 1994	Pier Base Shear/W_d	2	0.207	0.09	0.189	0.075	0.185	0.068	0.179	0.061		
		2.5	0.155	0.078	0.145	0.069	0.140	0.061	0.125	0.058	1.264	0.473
		3	0.138	0.081	0.129	0.071	0.125	0.065	0.119	0.061		
	Acceleration at Mid-Span (g)	2	0.229	0.141	0.211	0.125	0.189	0.118	0.181	0.111		
		2.5	0.188	0.121	0.181	0.118	0.175	0.111	0.169	0.098	0.919	0.518
		3	0.167	0.118	0.162	0.112	0.159	0.103	0.142	0.095		
	Displacement at Pier (m)	2	0.151	0.047	0.143	0.035	0.141	0.031	0.138	0.028		
		2.5	0.195	0.051	0.178	0.044	0.169	0.039	0.158	0.033	0	0
		3	0.225	0.066	0.215	0.053	0.200	0.048	0.188	0.042		
	Displacement at Abutment (m)	2	0.178	0.046	0.165	0.038	0.158	0.032	0.149	0.028		
		2.5	0.195	0.058	0.186	0.046	0.175	0.038	0.171	0.031	0	0
		3	0.221	0.069	0.205	0.055	0.195	0.045	0.189	0.039		
Kobe, 1995	Pier Base Shear/W_d	2	0.24	0.17	0.230	0.16	0.21	0.14	0.20	0.14		
		2.5	0.121	0.11	0.111	0.105	0.098	0.096	0.096	0.095	2.858	1.533
		3	0.10	0.18	0.088	0.165	0.079	0.138	0.071	0.129		
	Acceleration at Mid-Span (g)	2	0.28	0.20	0.26	0.18	0.230	0.17	0.230	0.16		
		2.5	0.245	0.155	0.238	0.148	0.225	0.141	0.220	0.138	2.158	1.619
		3	0.221	0.125	0.215	0.118	0.205	0.111	0.200	0.101		
	Displacement at Pier (m)	2	0.28	0.18	0.27	0.16	0.24	0.15	0.24	0.14		
		2.5	0.37	0.24	0.355	0.225	0.349	0.212	0.341	0.208		
		3	0.42	0.31	0.403	0.285	0.395	0.279	0.389	0.271		
	Displacement at Abutment (m)	2	0.31	0.16	0.27	0.14	0.24	0.13	0.24	0.12		
		2.5	0.38	0.23	0.36	0.215	0.351	0.201	0.345	0.198		
		3	0.46	0.27	0.44	0.255	0.431	0.249	0.427	0.233		

Table 6: Peak response quantities for the RC bridge with different controller schemes for foundation with hard soil condition.

It is generally well-established phenomena that the SSI tends to affect the seismic response of the base-isolated bridges. Therefore, Tables 5 through 8 are provided to evaluate the effect of the SSI on the performance of the hybrid systems such as, IB+STMD, IB+2TMDs, and IB+3TMDs.

| Responses under Ground Motions | | T_b | Base-Isolated Bridge with | | | | | | | | Fixed-Base | |
| | | | IB | | IB+STMD | | IB+2TMDs | | IB+3TMDs | | | |
			N-S	E-W	N-S	E-W	N-S	E-W	N-S	E-W	N-S	E-W
Imperial Valley, 1940	Pier Base Shear/W_d	2	0.065	0.088	0.061	0.082	0.058	0.079	0.055	0.074		
		2.5	0.078	0.077	0.073	0.074	0.069	0.069	0.065	0.066	0.576	0.655
		3	0.088	0.073	0.085	0.070	0.080	0.065	0.077	0.075		
	Acceleration at Mid-Span (g)	2	0.122	0.184	0.120	0.180	0.113	0.171	0.103	0.167		
		2.5	0.133	0.155	0.129	0.150	0.120	0.142	0.105	0.137	0.663	0.802
		3	0.135	0.125	0.130	0.120	0.125	0.111	0.109	0.098		
	Displacement at Pier (m)	2	0.045	0.065	0.038	0.062	0.036	0.057	0.031	0.049		
		2.5	0.072	0.080	0.069	0.077	0.061	0.071	0.059	0.066	0	0
		3	0.115	0.088	0.109	0.085	0.101	0.079	0.097	0.071		
	Displacement at Abutment (m)	2	0.132	0.165	0.125	0.158	0.122	0.151	0.118	0.147		
		2.5	0.202	0.198	0.189	0.185	0.186	0.181	0.179	0.175	0	0
		3	0.280	0.200	0.268	0.188	0.261	0.184	0.257	0.177		
Northridge, 1994	Pier Base Shear/W_d	2	0.109	0.036	0.098	0.035	0.096	0.033	0.092	0.031		
		2.5	0.104	0.061	0.101	0.058	0.097	0.052	0.094	0.049	1.089	0.441
		3	0.098	0.068	0.100	0.066	0.096	0.061	0.095	0.058		
	Acceleration at Mid-Span (g)	2	0.189	0.109	0.182	0.098	0.178	0.094	0.171	0.086		
		2.5	0.178	0.118	0.175	0.106	0.171	0.100	0.165	0.092	0.356	0.477
		3	0.162	0.129	0.160	0.115	0.158	0.110	0.150	0.100		
	Displacement at Pier (m)	2	0.069	0.021	0.058	0.018	0.048	0.016	0.042	0.014		
		2.5	0.120	0.045	0.105	0.033	0.098	0.028	0.088	0.025	0	0
		3	0.150	0.062	0.133	0.052	0.122	0.048	0.111	0.041		
	Displacement at Abutment (m)	2	0.202	0.048	0.198	0.041	0.189	0.038	0.179	0.033		
		2.5	0.240	0.065	0.225	0.059	0.212	0.051	0.200	0.048	0	0
		3	0.295	0.095	0.281	0.085	0.279	0.078	0.271	0.074		
Kobe, 1995	Pier Base Shear/W_d	2	0.16	0.13	0.18	0.13	0.14	0.10	0.14	0.10		
		2.5	0.14	0.11	0.125	0.098	0.111	0.092	0.099	0.088	2.034	1.033
		3	0.11	0.09	0.101	0.085	0.095	0.082	0.090	0.078		
	Acceleration at Mid-Span (g)	2	0.18	0.15	0.19	0.15	0.14	0.13	0.14	0.13		
		2.5	0.15	0.13	0.14	0.12	0.125	0.108	0.121	0.100	1.903	1.019
		3	0.12	0.11	0.115	0.107	0.106	0.100	0.100	0.096		
	Displacement at Pier (m)	2	0.22	0.16	0.23	0.16	0.21	0.13	0.21	0.13		
		2.5	0.28	0.23	0.265	0.218	0.249	0.200	0.238	0.195		
		3	0.36	0.28	0.345	0.268	0.339	0.250	0.325	0.239		
	Displacement at Abutment (m)	2	0.26	0.19	0.23	0.14	0.21	0.11	0.21	0.11		
		2.5	0.45	0.38	0.431	0.349	0.428	0.333	0.415	0.321		
		3	0.61	0.55	0.551	0.538	0.545	0.526	0.539	0.518		

Table 7: Peak response quantities for the RC bridge with different controller schemes for foundation medium soil condition.

Responses under Ground Motions			Base-Isolated Bridge with							Fixed-Base	
			IB		IB+STMD		IB+2TMDs		IB+3TMDs		
		T_b	N-S	E-W	N-S	E-W	N-S	E-W	N-S	E-W	N-S	E-W
Imperial Valley, 1940	Pier Base Shear/W_d	2	0.049	0.064	0.042	0.061	0.039	0.057	0.035	0.051		
		2.5	0.066	0.071	0.061	0.068	0.058	0.061	0.055	0.058	0.478	0.465
		3	0.075	0.068	0.071	0.066	0.066	0.062	0.063	0.060		
	Acceleration at Mid-Span (g)	2	0.130	0.195	0.115	0.188	0.111	0.181	0.105	0.179		
		2.5	0.135	0.140	0.128	0.125	0.115	0.118	0.107	0.108	0.366	0.638
		3	0.138	0.123	0.129	0.120	0.122	0.111	0.118	0.103		
	Displacement at Pier (m)	2	0.026	0.039	0.024	0.033	0.021	0.028	0.019	0.022		
		2.5	0.046	0.055	0.042	0.053	0.038	0.048	0.033	0.039	0	0
		3	0.095	0.091	0.088	0.085	0.082	0.078	0.075	0.066		
	Displacement at Abutment (m)	2	0.155	0.182	0.145	0.177	0.140	0.171	0.132	0.164		
		2.5	0.218	0.205	0.200	0.189	0.189	0.179	0.182	0.175	0	0
		3	0.295	0.235	0.278	0.218	0.271	0.205	0.268	0.200		
Northridge, 1994	Pier Base Shear/W_d	2	0.072	0.027	0.068	0.024	0.065	0.022	0.059	0.018		
		2.5	0.068	0.033	0.063	0.028	0.059	0.022	0.056	0.017	0.639	0.33
		3	0.059	0.038	0.056	0.035	0.051	0.027	0.048	0.021		
	Acceleration at Mid-Span (g)	2	0.174	0.154	0.158	0.149	0.152	0.146	0.148	0.144		
		2.5	0.166	0.163	0.154	0.144	0.149	0.140	0.142	0.138	0.336	0.347
		3	0.155	0.175	0.149	0.140	0.142	0.135	0.139	0.134		
	Displacement at Pier (m)	2	0.039	0.012	0.034	0.01	0.03	0.009	0.022	0.008		
		2.5	0.080	0.028	0.072	0.025	0.068	0.018	0.065	0.016	0	0
		3	0.106	0.044	0.085	0.042	0.081	0.038	0.075	0.030		
	Displacement at Abutment (m)	2	0.213	0.051	0.205	0.050	0.195	0.045	0.188	0.039		
		2.5	0.255	0.065	0.248	0.058	0.235	0.050	0.228	0.041	0	0
		3	0.315	0.100	0.308	0.088	0.300	0.080	0.285	0.068		
Kobe, 1995	Pier Base Shear/W_d	2	0.15	0.13	0.15	0.12	0.08	0.09	0.08	0.09		
		2.5	0.125	0.10	0.105	0.098	0.098	0.088	0.092	0.085	1.034	0.833
		3	0.10	0.08	0.098	0.075	0.086	0.085	0.087	0.082		
	Acceleration at Mid-Span (g)	2	0.16	0.16	0.16	0.16	0.10	0.13	0.10	0.12		
		2.5	0.14	0.13	0.12	0.115	0.10	0.095	0.089	0.082	0.903	0.719
		3	0.11	0.10	0.10	0.098	0.095	0.087	0.085	0.078		
	Displacement at Pier (m)	2	0.22	0.16	0.19	0.16	0.17	0.14	0.17	0.14		
		2.5	0.30	0.25	0.29	0.235	0.281	0.228	0.275	0.218		
		3	0.42	0.33	0.41	0.268	0.400	0.255	0.385	0.245		
	Displacement at Abutment (m)	2	0.22	0.20	0.21	0.14	0.17	0.12	0.17	0.12		
		2.5	0.48	0.45	0.47	0.445	0.465	0.431	0.451	0.422		
		3	0.71	0.67	0.70	0.665	0.689	0.654	0.678	0.649		

Table 8: Peak response quantities for the RC bridge with different controller schemes for foundation with soft soil condition.

In this study, the term robust is used for such cases wherein the seismic effectiveness is reduced relatively insignificantly even when off-tuning occurs due the soil properties. It is found that installing the TMD schemes improved the performance of the base-isolated bridge with and without SSI effect considerations. In addition, it is seen that by changing the properties of the soil from hard

(Table 6) to soft (Table 8) the pier and abutment displacement of the isolated bridge are magnified. Also, the 2TMDs and 3TMDs are more robust in the seismic response control of the RC bridges as compared to the STMD.

Not only the displacement response is reduced by installing the TMDs, but also the base shear and acceleration are controlled significantly. This fact is confirmed through the detailed parametric investigation reported in Tables 5 through 8. More importantly, the situation where only the displacement response is controlled, the base shear and acceleration are not magnified. This is yet another advantage of using the TMDs in seismic response control of isolated RC bridges.

It is, therefore, concluded that the TMDs are effective in controlling the displacement response of the bridge in all the configurations considered. Also, the post-peak response reduces substantially when the TMDs are installed as compared to the uncontrolled bridge and the isolated bridge equipped with the STMD. In addition, it is concluded that the acceleration of the bridge is reduced by installing the TMD(s) in different schemes. Further, the multiple TMDs generally provide increased dynamic response reduction as compared to the STMD.

4 CONCLUSIONS

Multi-mode dynamic response control of the three-span base-isolated reinforced concrete (RC) bridge including soil-structure interaction (SSI) under earthquake is presented. Tuned mass dampers (TMDs) are installed for multi-mode response modification of the isolated RC bridge in the hybrid control system. Comparison of the seismic responses is made for the bridge installed with the single tuned mass damper (STMD), two tuned mass dampers (2TMDs), and three tuned mass dampers (3TMDs) installed at the mid-spans, under different real bi-directional earthquake excitations. The following conclusions are drawn from the results of the numerical study presented here:

1. Significant reduction in displacement is achieved by installing the TMD(s). TMDs are effective in controlling the displacement response of the RC bridge in the two configurations considered here.
2. The pier base shear and deck acceleration induced in the base-isolated RC bridge further reduced significantly in both the longitudinal and transverse directions upon installation of the TMD(s) in the three schemes studied here.
3. The post-peak response reduces substantially when the TMDs are installed as compared to the uncontrolled fixed-base and STMD cases.
4. Multiple TMDs are generally observed to provide improved dynamic response reduction as compared to the STMD.
5. The relative isolator displacement has reduced considerably in the base-isolated RC bridge when flexible foundation is modeled by considering the soil-structures interaction (SSI).
6. The soil type greatly affects the design parameters of the STMD and nTMDs schemes and seismic responses of the RC bridge with flexible foundation, and the nTMDs are more robust against variation to soil parameters as compared to the STMD.

References

Daniel, Y., Lavan, O., and Levy, R. (2012) "Multiple tuned mass dampers for multimodal control of pedestrian bridges", Journal of Structural Engineering, American Society of Civil Engineers (ASCE), 138(9), 1173-1178.

Debnath, N., Deb, S. K., and Dutta, A. (2015) "Multi-modal vibration control of truss bridges with tuned mass dampers and general loading", Journal of Vibration and Control, DOI: 10.1177/1077546315571172.

Dicleli, M. (2007) "Supplemental elastic stiffness to reduce isolator displacements for seismic-isolated bridges in near-fault zones", Engineering Structures, 29(5), 763-775.

Dicleli, M., and Buddaram, S. (2007) "Equivalent linear analysis of seismic-isolated bridges subjected to near-fault ground motions with forward rupture directivity effect", Engineering Structures, 29(1), 21-32.

Jangid, R. S. (2004) "Seismic response of isolated bridges" Journal of Bridge Engineering, American Society of Civil Engineers (ASCE), 9(2), 156-166.

Luu, M., Zabel, V., and Könke, C. (2012) "An optimization method of multi-resonant response of high-speed train bridges using TMDs", Finite Elements in Analysis and Design, 53, 13-23.

Matin, A., Elias, S., and Matsagar, V. (2014) "Seismic control of continuous span concrete bridges with multiple tuned mass dampers", Proceeding of Second European Conference on Earthquake Engineering and Seismology (2ECEES), Istanbul, Turkey.

Matin, A., Elias, S., and Matsagar, V. (2017) "Seismic response control of reinforced concrete bridges with soil-structure interaction", The Bridge and Structural Engineer, ING/IABSE, 47(1), 46-53.

Miguel, L. F. F., Lopez, R. H., Torii, A. J., Miguel, L. F. F., and Beck, A. T. (2016) "Robust design optimization of TMDs in vehicle-bridge coupled vibration problems", Engineering Structures, 126, 703-711.

Matsagar, V. A., and Jangid, R. S. (2006) "Seismic response of simply supported base-isolate bridge with different isolators", International Journal of Applied Science and Engineering, 4(1), 55-71.

Pisal, A.Y., and Jangid, R.S. (2016) "Vibration control of bridge subjected to multi-axle vehicle using multiple tuned mass friction dampers", International Journal of Advanced Structural Engineering, 8(2), 1-15.

Randall, S. E., Halsted, D. M., and Taylor, D. L. (1981) "Optimum vibration absorbers for linear damped systems", Journal of Mechanical Design, 103(12), 908-913.

Ribes-Llario, F., Velarte-Gonzalez, J.L., Perez-Garnes, J.L. and Real-Herráiz, J.I. (2016) "Study of vibrations in a short-span bridge under resonance conditions considering train-track interaction", Latin American Journal of Solids and Structures, 13(7), 1236-1249.

Spyrakos, C.C. (1990) "Assessment of SSI on the longitudinal seismic response of short span bridges", Construction and Building Materials, 4(4), 170-175.

Tongaonkar, N.P. and Jangid, R.S. (2003) "Seismic response of isolated bridges with soil–structure interaction", Soil Dynamics and Earthquake Engineering, 23, 287-302.